

ORIGINAL ARTICLE

Does volume perfusion computed tomography enable differentiation of metastatic and non-metastatic mediastinal lymph nodes in lung cancer patients? A feasibility study

Daniel Spira^a, Matthias Wecker^a, Sven Michael Spira^b, Jürgen Hetzel^c, Werner Spengler^c, Alexander Sauter^a, Marius Horger^a

^aDepartment of Diagnostic and Interventional Radiology, Eberhard-Karls-University, Hoppe-Seyler-Str. 3, 72076 Tübingen, Germany; ^bFinance Department, HEC Paris, 1, rue de la Libération, 78350 Jouy en Josas, France; ^cDepartment of Oncology, Hematology, Immunology, Rheumatology and Pulmonology, Eberhard-Karls-University, Otfried-Müller-Str. 10, 72076 Tübingen, Germany

Corresponding address: Daniel Spira, MD, Department of Diagnostic and Interventional Radiology, Eberhard-Karls-University, Hoppe-Seyler-Str. 3, 72076 Tübingen, Germany.
Email: daniel.spira@med.uni-tuebingen.de

Date accepted for publication 6 June 2013

Abstract

Objectives: To compare the perfusion characteristics of mediastinal lymph node metastases with those of non-metastatic nodes in patients with newly diagnosed lung cancer using volume perfusion computed tomography (VPCT). **Materials and methods:** Between January 2010 and October 2011, 101 patients with histologically confirmed, untreated lung cancer received a 40-s VPCT of the tumor bulk; 32/101 patients had evident hilar/mediastinal metastatic disease and 17/101 patients had proven non-metastasized lymph nodes within the VPCT scan range. Validation or exclusion of metastatic node involvement was proven by mediastinoscopy, biopsy, positron emission tomography imaging and/or unequivocal volume dynamics on follow-up computed tomography. A total of 45 metastases and 23 non-metastatic lymph nodes were found within the scan range and subsequently evaluated. Blood flow (BF), blood volume (BV) and K^{trans} were determined. Tumor volume was recorded as whole tumor volume. **Results:** In a comparison between metastatic and non-metastatic lymph nodes, we controlled for age, lymph node volume, lung tumor volume, lung tumor location, and histologic type effects and found no significant differences with respect to BF, BV, K^{trans} or heterogeneity in nodal perfusion ($P > 0.05$, respectively), even after adjusting lymph node perfusion values to the perfusion parameters of the primary tumor ($P > 0.05$, respectively). Metastatic lymph node volume had a significant increasing effect on perfusion heterogeneity ($P < 0.05$, respectively) and BV in the primary was a highly significant factor for BV in metastatic disease ($P < 0.001$). **Conclusion:** Perfusion characteristics of mediastinal metastatic and non-metastatic lymph nodes in untreated lung cancer show considerable overlap, so that a reliable differentiation via VPCT is not possible.

Keywords: Lung cancer; metastasis; volume perfusion CT; VPCT; K^{trans} .

Introduction

Lung cancer constitutes the leading cause of cancer deaths in the United States^[1] and occurs mainly in 2 forms: small cell lung cancer (SCLC, about 15% of lung cancers) and non-small cell lung cancer (NSCLC,

about 85%). NSCLC encompasses 3 major histologic subtypes: squamous cell carcinoma (SCC), adenocarcinoma (Adeno-Ca), and large cell lung cancer (LCLC). Attempts have been made to characterize these tumor types with molecular techniques^[2], histopathology^[3], as well as anatomic and functional imaging via positron

emission tomography (PET), computed tomography (CT), and magnetic resonance imaging (MRI)^[4]. Recently, public attention has been drawn to perfusion imaging and especially the applicability and potential benefit of volume perfusion CT (VPCT) in the assessment of lung cancer^[5–7].

VPCT measures the accumulation of contrast material in a defined volume of interest (VOI) through repeated CT scanning. The density/time curves of the afferent artery and the VOI are compared, assuming that contrast pharmacokinetics correspond to a two-compartment model (Patlak analysis). This allows the estimation of perfusion and permeability in a tumor volume^[8]. Initially, intravascular contrast enhancement is used to assess perfusion^[9,10], whereas the subsequent permeation of contrast material from the intra- into the extravascular compartment can be used to measure the transit constant (K^{trans} or flow extraction product, which is the sum of capillary permeability and microvascular flow)^[11,12].

Although several studies have investigated the perfusion parameters and K^{trans} of primary pulmonary tumors^[5,6,13,14], no comparative assessment of mediastinal metastatic disease in lung cancer via VPCT has been described in the literature. Therefore, we set out to compare perfusion parameters, including K^{trans} (flow extraction product), in mediastinal metastatic disease and non-metastatic lymph nodes of newly diagnosed patients with lung cancer using VPCT. In the search for distinctive perfusion traits, 2 evaluations are necessary: First, we compare absolute VPCT values of metastatic and normal lymph nodes. In certain types of metastases such as lung metastases, perfusion characteristics in metastatic disease might be influenced by the respective primary. This may be less likely in lymph node metastasis, as lymph nodes could also be partially occupied by cancer cells. Nevertheless, it is reasonable to perform a second, additional analysis, adjusting lymph node perfusion values to the perfusion parameters of the respective primary tumor.

Materials and methods

Population

Our local Research Ethics Committee approved this study, and all patients provided written informed consent including information about the radiation exposure from the CT examinations. For eligibility, patients needed to have untreated, histologically confirmed lung cancer. Exclusion criteria for contrast medium administration were kidney dysfunction (i.e. a serum creatinine level $>150 \mu\text{mol/l}$), hypersensitivity to iodine-containing contrast material, pregnancy, and/or untreated hyperthyroidism. Between January 2010 and October 2011, 101 consecutive patients with histologically confirmed lung cancer were prospectively assessed. In due consideration

of radiation hygiene, the VPCT scan range of our feasibility study was limited to the primary and the lymph nodes contained within the same height, deliberately abstaining from complete mediastinal VPCT assessment. Histologic diagnosis of lung cancer was obtained by tumor resection and by core biopsy (using a true-cut 18–20 gage coaxial needle system). In 32/101 patients, metastatic disease within the VPCT scan range was shown by (a) core biopsy ($n=5$), (b) a pronounced reduction ($n=17$) or (c) increase in volume ($n=2$) without an inflammatory cause, and (d) [¹⁸F]fluorodeoxyglucose (FDG)-PET/CT ($n=8$). The criteria for metastatic disease were for (b) a volume reduction of $>50\%$ after onset of chemotherapy at CT surveillance ≤ 7 months, (c) a volume increase of $>50\%$ over a period of ≤ 6 months, (d) maximum standardized uptake value (SUV_{max}) >3.0 and a reduction in tumor volume of $>50\%$ under chemotherapy at follow-up ($n=4/8$); or masses $>4 \text{ cm}$ and SUV_{max} values of $5.6\text{--}10.8$ ($n=4/8$)^[15]. A total of 45 proven metastases in these 32 patients were found within the scan range and subsequently evaluated.

Analogously, in 17/101 patients, mediastinal metastatic disease was excluded in lymph nodes within the VPCT scan range by (a) resection ($n=8$) or (b) unchanged size at >6 months follow-up without any heterogeneity ($n=9$). Altogether 23 non-metastatic lymph nodes in these 17 patients were within the scan range; 2/49 patients had a combination of metastatic and non-metastatic nodes.

CT protocol

All examinations were performed on a 128-row CT scanner (Somatom Definition AS+, Siemens Healthcare, Forchheim, Germany). A non-enhanced low-dose CT (NECT) of the thorax (40 mAs, 100 kV, slice thickness = 5.0 mm, collimation $128 \times 0.6 \text{ mm}$, tube rotation time 0.5 s, pitch 0.6) was obtained to localize lung tumors. Subsequently, an experienced radiologist analyzed the NECT and a scan range of 6.9 cm z-axis coverage was planned over the lung cancer, followed by a VPCT of the tumor using an adaptive spiral scanning technique. Perfusion parameters were 80 kV, 60/80 mAs (for patients $<70 \text{ kg}$ and $>70 \text{ kg}$, respectively), collimation $64 \times 0.6 \text{ mm}$ with z-flying focal spot and 26 CT whole coverage of the lung cancer (1 scan every 1.5 s) within a total scan time of 40 s. The mean radiation exposure for perfusion measurements in the thorax was 3.0 mSv for a normal-weighted male and 5.5 mSv for a normal-weighted female^[16]. During perfusion scanning, the patients were asked to resume shallow breathing for the duration of the study. Fifty milliliters of Ultravist 370 (Bayer Vital Leverkusen, Germany) were injected at a flow rate of 5 ml/s in an antecubital vein followed by a saline flush of 50 ml NaCl at 5 ml/s, and a start delay of 4 s. Contrast medium was administered by using a dual-head pump injector (Stellant, Medtron, Saarbruecken,

Germany). After the perfusion scans, another 80 ml of contrast medium were applied, and dose-reduced (CARE dose) chest and abdominal CT scans were subsequently obtained for staging purposes. From the VPCT raw data, one set of axial images with a slice thickness of 3 mm for perfusion analysis was reconstructed without overlap, using a medium smooth tissue convolution kernel (B10f). All images were transferred to an external workstation (Multi-Modality Workplace, Siemens) for analysis.

Quantitative perfusion assessment

Data evaluation was performed with the syngo Volume Perfusion CT Body software based on Patlak analysis. The reader (a radiologist with 4 years of experience and with a focus on oncologic imaging for 3 years) was blinded to all clinical data except gender and age of the patients. Automated motion correction and noise reduction of the datasets were applied by using an integrated motion correction algorithm with non-rigid deformable registration for anatomic alignment^[17]. A VOI was drawn manually around the entire tumor or lymph node volumes in all 3 planes on the maximum intensity projection (MIP) image sets. Care was taken to exclude adjacent tissues and blood vessels. In the acquired dataset, a region of interest (ROI) was placed inside the aorta to measure the arterial input function and enable triggering of data evaluation. Perfusion parameter maps for blood flow (BF; ml/100 ml/min), blood volume (BV; ml/100 ml) and K^{trans} (ml/100 ml/min) were obtained for statistical analysis. Additional VOIs within the volume of the original VOIs, surrounding the area of maximum BF and maximum K^{trans} were drawn and values were recorded as BF_{max} and $K_{\text{max}}^{\text{trans}}$, respectively. Analogous to PET imaging studies using a ratio of maximum and mean SUV, the ratios of maximum and mean values within tumor masses were recorded to assess tumor heterogeneity with respect to BF and K_{trans} ^[18].

Lung cancer and lymph node volumes

Tumor volumes were determined in the standard contrast-enhanced CT scans by manual placement of a VOI around the tumor (using the Siemens Oncology/Volumetry tool on a dedicated workstation). The minimum long and short axis diameters of the lymph nodes were 8 mm and 5 mm, respectively. A lung tumor was defined as central when it had contact with the lung hilus^[19].

Statistics

All data are reported as the arithmetic mean \pm SD. Statistical analysis (software: Stata 11.0; StataCorp LP) was performed using the Student *t* test. Simple ordinary least squares (OLS) regressions were applied to estimate potential effects and controlled for age of lung tumor volume, lymph node volume, central versus peripheral location of the lung tumor, and tumor type. For all tests *P* values < 0.05 were considered as statistically significant.

Results

Location, histological subtypes and volume of lung cancers

Lung cancers were located centrally in 22/32 (69%) patients with metastatic disease and in 9/17 (53%) patients with excluded metastasis. Adeno-Ca was more frequently accompanied by normal lymph nodes, whereas SCLC was more often associated with node metastases (Table 1). Metastatic and non-metastatic nodes were evenly distributed in SCC (Table 1).

According to the Student *t* test, lung cancer tumor volume was just not significantly higher in patients with metastasis (81.8 ± 73.5 ml) compared with those in whom metastatic disease was excluded (41.4 ± 52.2 ml) ($P = 0.062$). Metastases had a mean volume of 26.4 ± 28.9 ml, whereas non-metastasized lymph nodes were considerably smaller (1.9 ± 2.4 ml) ($P < 0.001$).

Comparison of lymph node perfusion parameters in metastatic versus non-metastatic nodes

Even though perfusion parameters of metastatic lymph nodes seemed smaller than those of normal lymph nodes (Tables 2 and 3), these differences were not significant in our patient group due to a large overlap of values ($P > 0.05$). We studied the mets vs benign coefficient, which measures the difference of the various perfusion parameters between metastatic and normal lymph nodes. In an OLS regression of metastatic and normal lymph nodes, we controlled for age, lymph node volume, lung tumor volume, lung tumor location and tumor type effects, and found no significant differences with respect to either mean BF, mean BV, mean K^{trans} , the ratio of BF_{max} to mean BF (or the ratio of $K_{\text{max}}^{\text{trans}}$ to mean K^{trans} (Table 2) ($P > 0.05$, respectively).

Table 1 Patient characteristics

Patients	SCC	Adeno-Ca	SCLC	LCLC
Female/male	5/11	5/17	3/5	1/0
Age, years (range)	64 (50–84)	63 (42–83)	61 (47–79)	50
Proven metastatic disease, no. (%)	11/32 (34)	14/32 (44)	7/32 (22)	0/32 (0)
Metastatic disease excluded, no. (%)	6/17 (35)	9/17 (53)	1/17 (6)	1/17 (6)

Table 2 Perfusion parameters of primary lung tumors and mediastinal lymph nodes

	Mean BF (ml/100 ml/min)	Mean BV (ml/100 ml)	Mean K^{trans} (ml/100 ml/min)	BF_{max}/BF_{mean}	$K_{max}^{trans}/K_{mean}^{trans}$
Metastatic LN	33.1 ± 11.9	6.8 ± 4.0	23.7 ± 9.4	1.7 ± 0.53	1.8 ± 0.53
Non-metastatic LN	39.0 ± 20.1	8.8 ± 4.3	29.6 ± 14.9	1.3 ± 0.42	1.3 ± 0.48
Primary lung tumor	30.1 ± 13.6	7.0 ± 6.0	22.7 ± 10.6	2.1 ± 0.8	2.0 ± 0.7

This table presents the mean perfusion values ± SD of metastatic and non-metastatic mediastinal lymph nodes (LN) as well as primary lung tumors.

Table 3 Regression analysis of lymph node perfusion parameters in metastatic versus non-metastatic nodes

Dependent variable	Mean BF (ml/100 ml/min)	Mean BV (ml/100 ml)	Mean K^{trans} (ml/100 ml/min)	BF_{max}/BF_{mean}	$K_{max}^{trans}/K_{mean}^{trans}$
Intercept	38.303 [15.118]***	6.463 [3.990]	33.615 [11.112]	1.626 [0.413]***	2.305 [0.473]***
Mets vs benign	1.895 [4.799]	1.148 [1.267]	1.507 [3.528]***	-0.135 [0.131]	-0.275 [0.150]*
Age (years)	-0.032 [0.206]	0.009 [0.054]	-0.105 [0.152]	-0.002 [0.006]	-0.010 [0.006]
Lung tumor volume (ml)	-0.019 [0.032]	-0.004 [0.008]	-0.016 [0.024]	0.002 [0.001]**	-0.000 [0.001]
Lymph node volume (ml)	-0.132 [0.090]	-0.045 [0.024]*	-0.118 [0.066]*	0.009 [0.002]***	0.008 [0.003]***
Central Tu	2.457 [4.967]	0.418 [1.311]	3.831 [3.651]	-0.076 [0.136]	-0.029 [0.155]
Tumor type1	2.008 [5.149]	1.850 [1.359]	1.159 [3.785]	-0.268 [0.141]*	-0.237 [0.161]
Tumor type2	-1.036 [6.221]	2.349 [1.642]	-5.989 [4.573]	-0.331 [0.170]*	-0.095 [0.196]
Tumor type3	-5.236 [16.595]	-0.790 [4.380]	-10.966 [12.198]	-0.131 [0.454]	0.121 [0.519]
Observations	68	68	68	68	68
R ²	0.0851	0.1566	0.1679	0.4238	0.3153

This table presents OLS regressions for patients with Adeno-Ca, SCC, SCLC, and LCLC. The following are dummy variables. mets vs benign is coded 1 to indicate patients with non-metastasized nodes and is coded 0 to indicate patients with metastatic nodes. Central Tu is coded 1 if the tumor is located centrally. Tumor type1, tumor type2 and tumor type3 are coded 1 if the patient has SCC, SCLC, or LCLC, respectively. Hence, the baseline scenario represents patients with Adeno-Ca, and is coded by setting all 3 dummy variables to zero. Intercept coefficients are listed for the sake of completeness with no clinical relevance. ***, ** and * denote significance level at the 1, 5 and 10% levels, respectively.

Comparison of relative lymph node-to-lung tumor perfusion parameters in metastatic versus non-metastatic disease

Perfusion characteristics of the lung tumor itself might have an impact on perfusion values in metastatic disease. We therefore adjusted lymph node perfusion values to perfusion parameters of the respective primary tumor by calculating their ratio (Tables 2 and 4). However, when comparing metastatic with non-metastatic disease, after controlling for age, lymph node volume, lung tumor volume, lung tumor location, and tumor type effects, we found no significant differences concerning either mean BF (metastasis, 1.24 ± 0.69 ; non-metastasis, 1.44 ± 0.88), mean BV (metastasis, 1.38 ± 0.81 ; non-metastasis, 2.36 ± 4.16), mean K^{trans} (metastasis, 1.23 ± 0.58 ; non-metastasis, 1.32 ± 0.92), the ratio of BF_{max} to mean BF (metastasis, 0.88 ± 0.30 ; non-metastasis, 0.83 ± 0.36), or the ratio of K_{max}^{trans} to mean K^{trans} (metastasis, 0.91 ± 0.26 ; non-metastasis, 0.76 ± 0.33) ($P > 0.05$, respectively). Although no factor was found to be significant, the explanatory variables can explain between 8.2% and 19.4% of the variation in the perfusion parameters.

Regression analysis of lymph node perfusion parameters within groups

OLS regressions were performed to search for explanatory variables for mean BF and mean K^{trans} in metastatic

lymph nodes. No significance for any of the factors (age, lymph node volume, lung tumor volume, lung tumor location, and tumor type) was found ($P > 0.05$, respectively) (Table 5). However, in metastatic disease, lymph node volume had a significant increasing effect on the ratios BF_{max}/BF_{mean} and $K_{max}^{trans}/K_{mean}^{trans}$ ($P < 0.05$, respectively) (Table 5). Perfusion values of metastatic lymph nodes did not explain the perfusion parameters of the respective primary lung tumor, except for mean BV in the primary, which was a highly significant factor for mean BV in metastatic disease ($P < 0.001$) (Table 5).

Due to the smaller sample size, the analysis of non-metastatic lymph nodes had to be limited to a diminished set of explanatory variables. Thus, the same dependent variables were regressed on the respective perfusion parameters, as well as tumor volume of the primary and lymph node volume. No factor was found to be significant ($P > 0.05$, respectively) (Table 6).

Discussion

In patients with lung cancer without distant metastasis, mediastinal lymph node status is of major importance for appropriate treatment, as mediastinal spread (N2 and N3 disease) precludes a primarily surgical approach^[20]. CT, PET, PET/CT, mediastinoscopy, and needle aspiration techniques such as endobronchial ultrasonography (EBUS), esophageal ultrasonography (EUS), trans-bronchial needle aspiration and trans-thoracic needle

Table 4 Regression analysis of relative lymph node-to-lung tumor perfusion parameters in metastatic versus non-metastatic disease

Dependent variable	Mean BF (ml/100 ml/min)	Mean BV (ml/100 ml)	Mean K^{trans} (ml/100 ml/min)	BF_{max}/BF_{mean}	$K^{trans}_{max}/K^{trans}_{mean}$
Intercept	2.112 [0.753]***	-0.306 [2.446]	2.163 [0.691]***	0.452 [0.309]	0.981 [0.274]***
Mets vs benign	0.151 [0.239]	0.770 [0.777]	0.026 [0.219]	-0.013 [0.098]	-0.132 [0.087]
Age (years)	-0.010 [0.010]	0.019 [0.033]	-0.009 [0.009]	0.006 [0.004]	-0.003 [0.004]
Lung tumor volume (ml)	-0.000 [0.002]	-0.001 [0.005]	-0.001 [0.001]	0.001 [0.001]	-0.000 [0.001]
Lymph node volume (ml)	-0.001 [0.004]	-0.008 [0.015]	-0.001 [0.004]	0.003 [0.002]	0.002 [0.002]
Central Tu	-0.444 [0.247]*	0.498 [0.804]	-0.364 [0.227]	0.137 [0.102]	0.129 [0.090]
Tumor type1	0.145 [0.257]	1.330 [0.833]	-0.185 [0.235]	-0.072 [0.105]	0.007 [0.093]
Tumor type2	0.274 [0.310]	0.316 [1.007]	0.066 [0.284]	-0.177 [0.127]	-0.096 [0.113]
Tumor type3	0.123 [0.827]	0.473 [2.685]	-0.366 [0.759]	-0.042 [0.340]	0.304 [0.301]
Observations	68	68	68	68	68
R^2	0.0818	0.1202	0.1133	0.1271	0.1939

This table presents OLS regressions for patients with Adeno-Ca, SCC, SCLC, and LCLC. The following are dummy variables. Mets vs benign" is coded 1 to indicate patients with non-metastasized nodes and is coded 0 to indicate patients with metastatic nodes. Central Tu is coded 1 if the tumor is located centrally. Tumor type1, tumor type2 and tumor type3 are coded 1 if patient has SCC, SCLC, or LCLC, respectively. Hence, the baseline scenario represents patients with Adeno-Ca, and is coded by setting all 3 dummy variables to zero. Intercept coefficients are listed for the sake of completeness with no clinical relevance. ***, ** and * denote significance level at the 1, 5 and 10% levels, respectively.

Table 5 Regression analysis of lymph node perfusion parameters in metastatic nodes

Dependent variable	Mean BF (ml/100 ml/min) (LN)	Mean BV (ml/100 ml) (LN)	Mean K^{trans} (ml/100 ml/min) (LN)	BF_{max}/BF_{mean} (LN)	$K^{trans}_{max}/K^{trans}_{mean}$ (LN)
Intercept	31.4873 [12.880]**	4.343 [3.540]	22.560 [9.844]**	1.116 [0.592]*	1.694 [0.653]**
BF_{BC} (ml/100 ml/min)	0.210 [0.172]	—	—	—	—
BV_{BC} (ml/100 ml)	—	0.594 [0.131]***	—	—	—
K^{trans}_{BC} (ml/100 ml/min)	—	—	0.313 [0.237]	—	—
$BF_{Ratio BC}$	—	—	—	0.162 [0.097]	—
$K^{trans}_{Ratio BC}$	—	—	—	—	0.220 [0.132]
Age (years)	-0.007 [0.026]	-0.015 [0.050]	-0.007 [0.139]	0.000 [0.007]	-0.009 [0.007]
LT volume (ml)	-0.014 [0.026]	-0.001 [0.007]	-0.008 [0.020]	0.002 [0.001]*	0.000 [0.001]
LN volume (ml)	-0.094 [0.074]	-0.034 [0.020]	-0.080 [0.055]	0.008 [0.003]**	0.006 [0.003]**
Central Tu	-2.327 [5.168]	-0.631 [1.344]	-2.774 [3.910]	0.036 [0.195]	0.122 [0.196]
Tumor type1	0.921 [5.137]	2.518 [1.428]*	0.594 [3.848]	-0.270 [0.184]	-0.148 [0.207]
Tumor type2	1.869 [5.775]	2.523 [1.511]	-2.774 [3.910]	-0.331 [0.196]	-0.087 [0.218]
Observations	45	45	45	45	45
R^2	0.1367	0.4256	0.2254	0.4419	0.3140

This table presents OLS regressions for patients with Adeno-Ca, SCC, and SCLC. BF_{BC} , lung cancer mean BF; BV_{BC} , lung cancer mean BC; K^{trans}_{BC} , lung cancer mean K^{trans} ; $BF_{Ratio BC}$, lung cancer BF_{max}/BF_{mean} ; $K^{trans}_{Ratio BC}$, lung cancer $K^{trans}_{max}/K^{trans}_{mean}$. The following are dummy variables: Central Tu is coded 1 if the tumor is located centrally. Tumor type1 and tumor type2 are coded 1 if the patient has SCC or SCLC, respectively. Hence, the baseline scenario represents patients with Adeno-Ca, and is coded by setting both dummy variables equal to zero. Intercept coefficients are listed for the sake of completeness with no clinical relevance. ***, ** and * denote significance level at the 1, 5 and 10% levels, respectively.

aspiration are used for mediastinal staging^[21]. Although the use of PET and PET/CT combined with well-directed EBUS and EUS increases sensitivities, specificities, and accuracies to >90%^[22,23], the diagnostic accuracy for CT, PET and even PET/CT alone is low in an unselected population^[15,24]. Hence, new imaging techniques capturing tissue characteristics other than size or metabolic activity may enable further improvement in the depiction of metastases and are still being searched for.

Tumor angiogenesis results in the formation of tortuous, irregular and immature blood vessels. These neovessels demonstrate an incomplete basement membrane,

defects in the endothelial cell layer and transcellular holes^[25,26]. The consecutive net efflux of fluid into the surrounding interstitial space and the lack of functional lymphatics leads to increased interstitial pressure^[27,28]. Extracellular matrix remodeling by fibroblasts, macrophages and other inflammatory cells further contributes to increased interstitial pressure but also forms a barrier to transcapillary transport. These pathophysiologic changes create an obstacle for treatment of tumors through inefficient uptake of therapeutic agents^[29] and may result in characteristic traits concerning tumor vascularization and permeability.

Table 6 Regression analysis of lymph node perfusion parameters in non-metastatic nodes

Dependent variable	Mean BF (ml/100 ml/min) (LN)	Mean BV (ml/100 ml) (LN)	Mean K^{trans} (ml/100 ml/min) (LN)	BF_{max}/BF_{mean} (LN)	$K_{max}^{trans}/K_{mean}^{trans}$ (LN)
Intercept	28.966 [12.745]**	10.281 [2.048]***	18.955 [9.079]*	1.104 [0.241]***	1.323 [0.264]***
BF_{BC} (ml/100 ml/min)	0.325 [0.345]	—	—	—	—
BV_{BC} (ml/100 ml)	—	-0.054 [0.135]	—	—	—
K_{BC}^{trans} (ml/100 ml/min)	—	—	0.337 [0.257]	—	—
$BF_{Ratio\ BC}$	—	—	—	0.050 [0.151]	—
$K_{Ratio\ BC}^{trans}$	—	—	—	—	0.007 [0.102]
LT volume (ml)	-0.009 [0.082]	-0.007 [0.018]	0.033 [0.060]	0.000 [0.002]	-0.001 [0.002]
LN volume (ml)	0.184 [1.965]	-0.348 [0.415]	0.157 [1.433]	0.066 [0.039]	0.021 [0.047]
Observations	23	23	23	23	23
R^2	0.0454	0.0513	0.0885	0.1953	0.0319

This table presents OLS regressions for patients with Adeno-Ca, SCC, SCLC, and LCLC. BF_{BC} , lung cancer mean BF; BV_{BC} , lung cancer mean BV; K_{BC}^{trans} , lung cancer mean K^{trans} ; $BF_{Ratio\ BC}$, lung cancer BF_{max}/BF_{mean} ; $K_{Ratio\ BC}^{trans}$, lung cancer $K_{max}^{trans}/K_{mean}^{trans}$. Intercept coefficients are listed for the sake of completeness with no clinical relevance. ***, ** and * denote significance level at the 1, 5 and 10% levels, respectively.

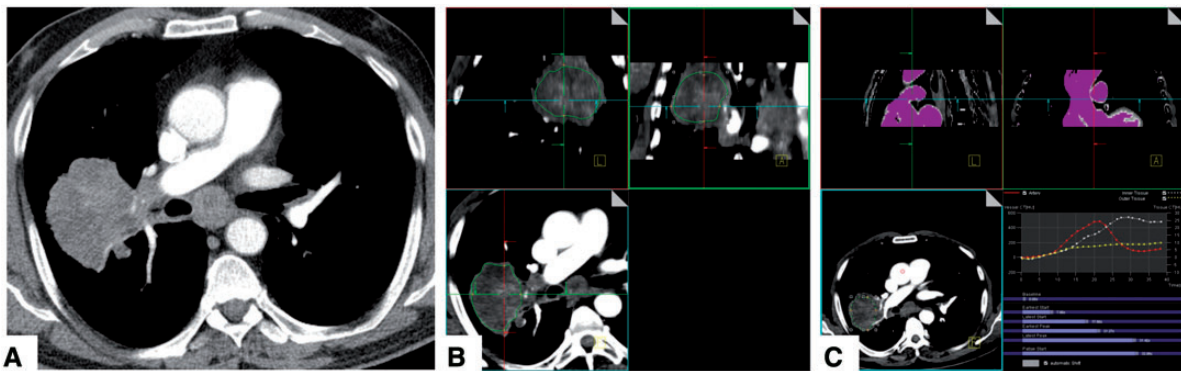


Figure 1 Contrast-enhanced CT shows an adenocarcinoma of the right upper lobe with contact with the hilus (A). In the VPCT data set (MIP reconstructions), a VOI is drawn manually around the entire tumor volume in all 3 planes (B). An ROI is placed inside the ascending aorta to obtain the arterial input function (C).

VPCT using new-generation multidetector CT scanners and automated motion correction allow for high spatial and temporal resolution by close-meshed scanning sequences, even with free shallow breathing of the patient. Conflicting results exist concerning the value of perfusion imaging in the depiction of malignant lymph nodes, depending on lymph node location and the tumor being studied. Razek et al.^[30] detected significant differences in the mean dynamic susceptibility contrast (DSC) percentage of benign and metastatic cervical lymph nodes from SCC, using MR perfusion imaging. In contrast, Bisdas et al.^[31] observed that perfusion values and permeability surface product as determined by VPCT were not significantly different in metastatic and non-metastatic lymph nodes in patients with oropharyngeal and oral cavity cancer. Liu et al.^[32] again found significant differences in BF (but not BV or permeability surface) via VPCT between metastatic and inflammatory enlarged axillary lymph nodes in patients with breast cancer. Hence, additional characteristics, such as vascularization and permeability of lymph nodes, may enable a further improvement in the diagnosis of lymph node metastasis.

This is the first study to investigate perfusion parameters, including K^{trans} in mediastinal metastatic disease and non-metastatic lymph nodes in patients with untreated lung cancer using VPCT. Even though the mean perfusion parameters of metastatic lymph nodes and primary lung tumors seemed smaller than those of non-metastatic lymph nodes, these differences were not significant in our patient group ($P > 0.05$). Consequently, in an OLS regression of metastatic and normal lymph nodes, we found no significant differences with respect to BF, BV, K^{trans} or heterogeneity in nodal perfusion but a broad range of values. Perfusion characteristics in solid metastatic disease might be influenced by the respective primary. Although this may be less likely in lymph node metastasis, we still performed a second analysis adjusting lymph node perfusion values to the perfusion parameters of the respective primary tumor. However, again, no significant differences in perfusion and K^{trans} of metastatic and non-metastatic disease were observed. Other studies have reported that large-sized lung cancers exhibit lower perfusion values compared with smaller tumors, probably due to central tumor necrosis and increased interstitial pressure^[19,33]. Concordantly, we found that

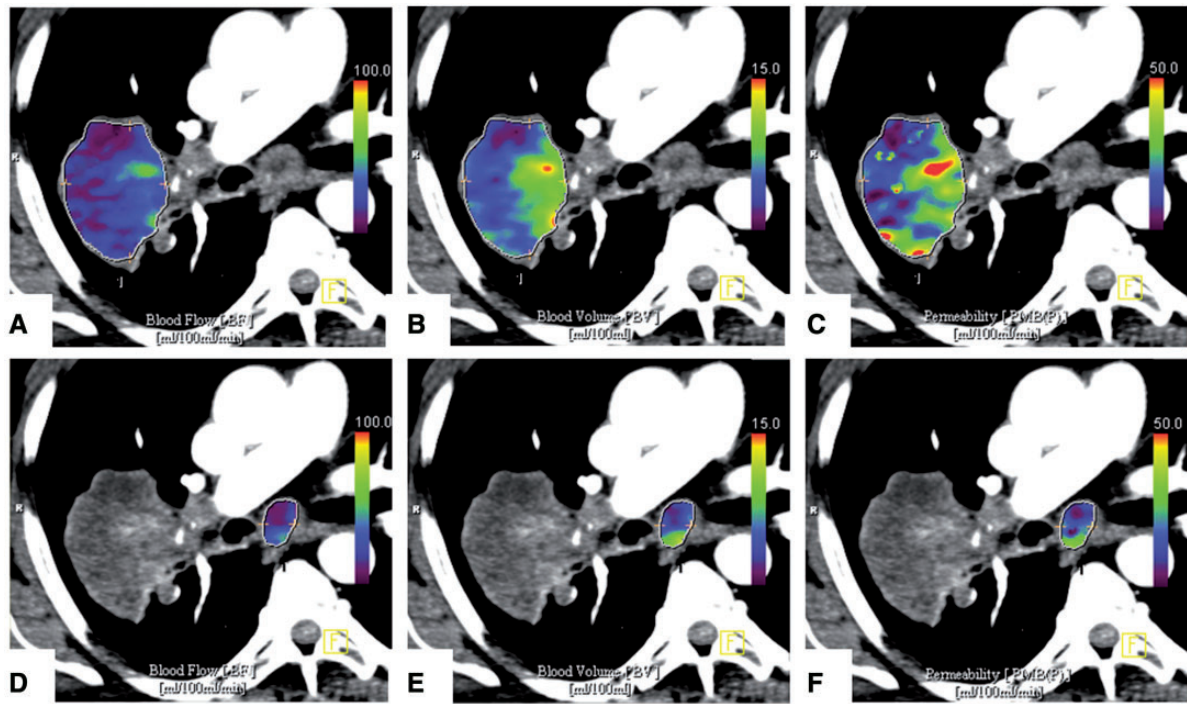


Figure 2 Perfusion parameter maps for BF (ml/100 ml/min), BV (ml/100 ml) and K^{trans} (ml/100 ml/min) of lung tumor (A–C) and mediastinal lymph node (D–E), respectively.

lymph node volume had a significantly increasing effect on perfusion heterogeneity. Perfusion values of metastatic lymph nodes were not explained by the perfusion parameters of the respective primary lung tumor, except for mean BV in the primary, which was a highly significant factor for mean BV in metastatic disease. However, this connection cannot be used to reliably differentiate between malignant and benign disease in lung cancer.

Our results for lung cancer metastasis to the mediastinum differ from those reported for oropharyngeal/hypopharyngeal cancer metastasis to the neck^[31] or breast cancer metastasis to the axilla^[32], where higher perfusion values are described in metastatic compared with normal lymph nodes. There are different possible explanations for this diversity, as well as the great overlap in perfusion of both metastatic and non-metastatic lymph nodes. Heterogeneity of perfusion within the metastatic group may reflect areas of necrosis^[19,33] or unspecific perfusion of the primary tumor^[34] and confirm the uniqueness of every single tumor, being influenced by many variables including the microenvironment. Furthermore, lung cancer and mediastinal metastatic disease are often diagnosed at a later stage and with larger tumor volumes than oropharyngeal cancer and neck metastasis or breast cancer and axillary metastasis. This is also reflected in our results where we find a mean tumor volume of mediastinal metastases of 26.4 ± 28.9 ml, which is much larger than the neck metastases of oropharyngeal cancer (5.19 ± 4.89 ml) described by Bisdas et al.^[31] or

the axillary metastases (mean diameter 1.60 ml) observed by Liu et al.^[32]. As larger tumors have a higher likelihood of becoming necrotic^[19,33], this may at least partially explain the differences in perfusion traits. Every tumor type has different characteristics and the results for oral, breast or lung cancer cannot be generalized to all other carcinomas. Non-metastatic mediastinal lymph node enlargement is believed to represent a reaction to infectious or immunologic processes passing through different phases of inflammatory activity. Thus, the coexistence of both active and inactive inflammation within these nodes may have a bearing on the degree of perfusion^[32,35]. Moreover, areas of post-stenotic pneumonia and impairment of mucociliary clearance are accompanied by some degree of inflammation, which may again affect lymph node perfusion. This is also thought to explain the false-positive and false-negative results of FDG-PET in this clinical setting^[15,24].

This study has several shortcomings. First, due to the small sample size, an in-depth regression analysis involving all variables was hampered in the non-metastatic lymph node group and the within-group analysis had to be conducted on a limited set of explanatory variables, as otherwise there was not enough variation in the dataset. Further studies are warranted to elucidate these interrelations. However, this was not the principle point of this study; the goal was to compare perfusion parameters of metastatic and non-metastatic lymph nodes in patients with untreated lung cancer and search for possible differentiating parameters. Second, not all mediastinal lymph

nodes were evaluated by VPCT. In due consideration of radiation hygiene, the VPCT scan range of our feasibility study was limited to the primary and the lymph nodes contained within the same height, deliberately abstaining from complete mediastinal VPCT assessment. Furthermore, the VPCT protocol does not allow for highly accurate BF measurement due to the limited temporal resolution chosen, dictated by the concern about dose exposure, which is inherent to any radiation-based technique.

Conclusion

Our preliminary results show that VPCT perfusion parameters and K^{trans} of metastatic and non-metastatic lymph nodes in patients with untreated lung cancer cover a broad range of values and cannot be used for reliable depiction of mediastinal disease.

Acknowledgements

We thank Nicole Sachse and Astrid Schreiber (Diagnostic and Interventional Radiology, Eberhard-Karls-University Tuebingen) for excellent technical assistance. We also thank Siemens Healthcare (Forchheim, Germany) for technical support.

Conflict of interest

Claus Detlef Claussen (head of the Department of Diagnostic and Interventional Radiology, Eberhard-Karls-University Tuebingen) received technical support from Siemens Healthcare (Forchheim, Germany). Otherwise, we herewith declare no conflicts of interest or financial disclosures for the authors of this manuscript.

References

- [1] Siegel R, Ward E, Brawley O, Jemal A. Cancer statistics, 2011: the impact of eliminating socioeconomic and racial disparities on premature cancer deaths. *CA Cancer J Clin* 2011; 61: 212–236. PMID:21685461.
- [2] Herbst RS, Heymach JV, Lippman SM. Lung cancer. *N Engl J Med* 2008; 359: 1367–1380. PMID:18815398.
- [3] Sardari Nia P, Van Marck E, Weyler J, Van Schil P. Prognostic value of a biologic classification of non-small-cell lung cancer into the growth patterns along with other clinical, pathological and immunohistochemical factors. *Eur J Cardiothorac Surg* 2010; 38: 628–636. PMID:20452237.
- [4] Rehman S, Jayson GC. Molecular imaging of antiangiogenic agents. *Oncologist* 2005; 10: 92–103. PMID:15709211.
- [5] Tacelli N, Remy-Jardin M, Copin MC, et al. Assessment of non-small cell lung cancer perfusion: pathologic-CT correlation in 15 patients. *Radiology* 2010; 257: 863–871. PMID:20843993.
- [6] Fraioli F, Anzidei M, Zaccagna F, et al. Whole-tumor perfusion CT in patients with advanced lung adenocarcinoma treated with conventional and antiangiogenic chemotherapy: initial experience. *Radiology* 2011; 259: 574–582. PMID:21357523.
- [7] Ng CS, Chandler AG, Wei W, et al. Reproducibility of perfusion parameters obtained from perfusion CT in lung tumors. *AJR Am J Roentgenol* 2011; 197: 113–121. PMID:21701018.
- [8] Petralia G, Preda L, D'Andrea G, et al. CT perfusion in solid-body tumours. Part I: technical issues. *Radiol Med* 2010; 115: 858–874. PMID:20221706.
- [9] Miles KA. Perfusion CT for the assessment of tumour vascularity: which protocol? *Br J Radiol* 2003; 76 (Spec No 1): S36–42. PMID:15456712.
- [10] Miles KA, Charnsangavej C, Lee FT, Fishman EK, Horton K, Lee TY. Application of CT in the investigation of angiogenesis in oncology. *Acad Radiol* 2000; 7: 840–850. PMID:11048881.
- [11] Petralia G, Preda L, D'Andrea G, et al. CT perfusion in solid-body tumours. Part I: technical issues. *Radiol Med* 2010; 115: 858–874. PMID:20221706.
- [12] Kambadakone AR, Sahani DV. Body perfusion CT: technique, clinical applications, and advances. *Radiol Clin North Am* 2009; 47: 161–178. PMID:19195541.
- [13] Yi CA, Lee KS, Kim EA, et al. Solitary pulmonary nodules: dynamic enhanced multi-detector row CT study and comparison with vascular endothelial growth factor and microvessel density. *Radiology* 2004; 233: 191–199. PMID:15304661.
- [14] Li Y, Yang ZG, Chen TW, Yu JQ, Sun JY, Chen HJ. First-pass perfusion imaging of solitary pulmonary nodules with 64-detector row CT: comparison of perfusion parameters of malignant and benign lesions. *Br J Radiol* 2010; 83: 785–790. PMID:20647512.
- [15] Perigaud C, Bridji B, Roussel JC, et al. Prospective preoperative mediastinal lymph node staging by integrated positron emission tomography-computerised tomography in patients with non-small-cell lung cancer. *Eur J Cardiothorac Surg* 2009; 36: 731–736. PMID:19632852.
- [16] Ketelsen D, Horger M, Buchgeister M, et al. Estimation of radiation exposure of 128-slice 4D-perfusion CT for the assessment of tumor vascularity. *Korean J Radiol* 2010; 11: 547–552. PMID:20808699.
- [17] Chandler A, Wei W, Anderson EF, Herron DH, Ye Z, Ng CS. Validation of motion correction techniques for liver CT perfusion studies. *Br J Radiol* 2012; 85: e514–e522. PMID:22374283.
- [18] Salamon J, Derlin T, Bannas P, et al. Evaluation of intratumoural heterogeneity on (18)F-FDG PET/CT for characterization of peripheral nerve sheath tumours in neurofibromatosis type 1. *Eur J Nucl Med Mol Imaging* 2013; 40: 685–692. PMID:23232507.
- [19] Kiessling F, Boese J, Corvinus C, et al. Perfusion CT in patients with advanced bronchial carcinomas: a novel chance for characterization and treatment monitoring? *Eur Radiol* 2004; 14: 1226–1233. PMID:15029450.
- [20] Fischer BM, Mortensen J, Hansen H, et al. Multimodality approach to mediastinal staging in non-small cell lung cancer. Faults and benefits of PET-CT: a randomised trial. *Thorax* 2011; 66: 294–300. PMID:21169287.
- [21] Detterbeck F, Puchalski J, Rubinowitz A, Cheng D. Classification of the thoroughness of mediastinal staging of lung cancer. *Chest* 2010; 137: 436–442. PMID:20133290.
- [22] Fidler MJ, Kim AW, Zusag T, Bonomi P. Treatment of locally advanced non-small cell lung cancer. *Clin Adv Hematol Oncol* 2009; 7: 455–464, 479–480. PMID:19701153.
- [23] Rintoul RC, Tournoy KG, El Daly H, et al. EBUS-TBNA for the clarification of PET positive intra-thoracic lymph nodes-an international multi-centre experience. *J Thorac Oncol* 2009; 4: 44–48. PMID:19096305.
- [24] Ozawa Y, Hara M, Sakurai K, et al. Diagnostic accuracy of (18)F-2-deoxy-fluoro-D-glucose positron emission tomography for pN2 lymph nodes in patients with lung cancer. *Acta Radiol* 2010; 51: 150–155. PMID:20092375.
- [25] Hashizume H, Baluk P, Morikawa S, et al. Openings between defective endothelial cells explain tumor vessel leakiness. *Am J Pathol* 2000; 156: 1363–1380. PMID:10751361.

- [26] Baluk P, Morikawa S, Haskell A, Mancuso M, McDonald DM. Abnormalities of basement membrane on blood vessels and endothelial sprouts in tumors. *Am J Pathol* 2003; 163: 1801–1815. PMID:14578181.
- [27] Milosevic M, Fyles A, Hedley D, Hill R. The human tumor micro-environment: invasive (needle) measurement of oxygen and interstitial fluid pressure. *Semin Radiat Oncol* 2004; 14: 249–258. PMID:15254868.
- [28] Lunt SJ, Kalliomaki TM, Brown A, Yang VX, Milosevic M, Hill RP. Interstitial fluid pressure, vascularity and metastasis in ectopic, orthotopic and spontaneous tumours. *BMC Cancer* 2008; 8: 2. PMID:18179711.
- [29] Heldin CH, Rubin K, Pietras K, Ostman A. High interstitial fluid pressure - an obstacle in cancer therapy. *Nat Rev Cancer* 2004; 4: 806–813. PMID:15510161.
- [30] Abdel Razek AA, Gaballa G. Role of perfusion magnetic resonance imaging in cervical lymphadenopathy. *J Comput Assist Tomogr* 2011; 35: 21–25. PMID:21245685.
- [31] Bisdas S, Baghi M, Smolarz A, et al. Quantitative measurements of perfusion and permeability of oropharyngeal and oral cavity cancer, recurrent disease, and associated lymph nodes using first-pass contrast-enhanced computed tomography studies. *Invest Radiol* 2007; 42: 172–179. PMID:17287647.
- [32] Liu Y, Bellomi M, Gatti G, Ping X. Accuracy of computed tomography perfusion in assessing metastatic involvement of enlarged axillary lymph nodes in patients with breast cancer. *Breast Cancer Res* 2007; 9: R40. PMID:17615058.
- [33] Miles KA, Griffiths MR, Keith CJ. Blood flow-metabolic relationships are dependent on tumour size in non-small cell lung cancer: a study using quantitative contrast-enhanced computer tomography and positron emission tomography. *Eur J Nucl Med Mol Imaging* 2006; 33: 22–28. PMID:16180030.
- [34] Basu S, Kwee TC, Gatenby R, Saboury B, Torigian DA, Alavi A. Evolving role of molecular imaging with PET in detecting and characterizing heterogeneity of cancer tissue at the primary and metastatic sites, a plausible explanation for failed attempts to cure malignant disorders. *Eur J Nucl Med Mol Imaging* 2011; 38: 987–991. PMID:21451997.
- [35] Goh V, Halligan S, Taylor SA, Burling D, Bassett P, Bartram CI. Differentiation between diverticulitis and colorectal cancer: quantitative CT perfusion measurements versus morphologic criteria—initial experience. *Radiology* 2007; 242: 456–462. PMID:17255417.